

Inverse Solution Uniqueness and Domain of Existence for Space-Marching Applications

Jae-Woo Lee*

Konkuk University, Seoul 143-701, Republic of Korea

and

W. H. Mason†

Virginia Polytechnic Institute and State University, Blacksburg, Virginia 24061

Inverse solution existence and uniqueness issues are discussed for supersonic and hypersonic three-dimensional inverse procedures that use space-marching techniques. By using extreme body-slope angle, a simple method to estimate the limiting domain of inverse solution existence is proposed and applied to several example test cases with and without angle of attack. The method provides useful information about possible target pressure distributions and inverse solution existence without performing any inverse calculations. By investigating the relations between the surface pressure and the body geometry, a general explanation for inverse solution uniqueness has been described. Sample calculations to support this explanation are presented.

Nomenclature

C_p	= pressure coefficient at the body surface
i, j, k	= indices of the computational plane
M_n	= Mach number normal to the shock wave
M_∞	= freestream Mach number
x, y, z	= physical coordinates: axial, spanwise, and vertical, respectively
y_{\max}	= planform shape
z_0	= reference point value
α	= angle of attack
γ	= ratio of specific heats
θ	= body-slope angle
θ_0	= body-slope angle obtained from the surface streamline
θ_1	= body-slope angle obtained from calculated pressure coefficient

Introduction

THE renewed interest in the design concepts for both the high-speed civil transport (HSCT) and space launchers, including reusable launch vehicles (RLV) and low-Earth-orbit (LEO) satellite launchers, may mark the beginning of a new era of advanced vehicles.^{1,2} Practical inverse design methods are needed for the speed range of these vehicles, and several have been developed recently. One method was established for axisymmetric flow³ and then extended to handle general three-dimensional⁴ bodies assuming that space-marching numerical procedures could be used. The methods were demonstrated using the Euler equations. Both methods have been shown to be robust and efficient.

Inverse methods require that the user have some design experience and appreciate the subtlety of aerodynamic design in order to specify a pressure distribution for which a geometry exists. (Aerodynamically attractive pressure distributions may require a physically unrealistic geometry or, in general, a geometry that is unattractive from the structural engineering standpoint). Because of the importance of the specification of the target pressure distribution in the inverse design problem, the issue of whether a unique solution (body geometry) exists for the given target pressure distribution must be considered in order to develop practical aerodynamic design methods.

The inverse solution existence and uniqueness problem was first raised by Lighthill.⁵ Using conformal mapping techniques in two-dimensional incompressible flow, he demonstrated that a unique and correct solution to the inverse problem does not exist unless the prescribed pressure (or, equivalently speed) distribution satisfies certain integral constraints. Two constraints arise from the requirement that the airfoil profile have a specific trailing-edge gap. A third, more subtle, constraint requires that the prescribed surface speed distribution be compatible with the specified freestream speed. Woods⁶ has pointed out that similar constraints are also required in the mixed design problem in which the pressure distribution is prescribed for some parts of the airfoil and the shape is prescribed elsewhere.

Volpe and Melnik^{7,8} have demonstrated that the role of constraints and the question of correct formulation of the inverse problem have never been properly addressed for two-dimensional compressible flow and that, as a consequence, most existing inverse methods for transonic flow are not well formulated. Similar constraints plausibly exist for compressible flow, at least in the absence of shock waves.⁸ The existence of these three constraints implies that in general the target speed distribution must contain three free parameters to guarantee that the constraints can be satisfied through proper adjustment of the parameters. Thus, the originally prescribed target pressure changes during the inverse design iterations to satisfy the constraints. Introducing a potential function to formulate these three constraints mathematically, Volpe and Melnik successfully applied the method to two-dimensional compressible potential flow. Because particular forms are needed for the functions⁹ that correct the target speed according to the constraints, it was not easy to apply the method for general two-dimensional flows. Thus, for compressible flow they pioneered the investigation of the existence of inverse solutions and formulated the constraint conditions mathematically.

A similar solution existence problem was studied by Daripa.¹⁰ He concentrated on the third constraint of Lighthill. The freestream Mach number obtained from the input pressure distribution using the irrotational and isentropic relations and Bernoulli's equation is compared with M_∞^C . (The computed freestream Mach number that is determined by the solution of the governing equations subject to the target pressure distribution.) For a solution to exist, M_∞ determined directly from the input C_p and the computed M_∞^C must be the same. Otherwise, a solution with the input pressure distribution does not exist. The other two constraints⁵ connected to the trailing-edge closure problem were not discussed.

The trailing-edge closure problem was investigated by Volpe and Melnik,⁷ Carlson and co-workers,^{11,12} and Shankar¹³ at the subsonic and transonic speeds. Prescription of an unconstrained pressure distribution may lead to the airfoil sections, which have either an excessively blunt trailing edge (open) or which, at least numerically,

Received 19 May 1998; revision received 9 June 1999; accepted for publication 8 July 1999. Copyright © 1999 by the American Institute of Aeronautics and Astronautics, Inc. All rights reserved.

*Assistant Professor, Department of Aerospace Engineering. Member AIAA.

†Professor, Department of Aerospace and Ocean Engineering. Associate Fellow AIAA.

have the upper and lower surfaces crossed at the trailing edge (fish-tailed). References 11 and 12 adjusted the nose radius (relofting) to close the trailing edge in his direct-inverse calculation. Shankar¹³ altered the velocity potentials in front of the leading edge to obtain automatic trailing-edge closure. Even though they ignored the role of the constraints derived by Lighthill⁵ and Woods,⁶ closed airfoils and wings were generated, and their methods are useful for the inverse problem in the subsonic and transonic flow.

All of the inverse methods just described have been developed for airfoils or wings in the subsonic and transonic potential flows and remain approximately valid even for the rotational flow when the shocks are relatively weak ($M_n < 1.2 \sim 1.3$). As pointed out by Moretti,¹⁴ it is necessary to abandon the potential equation and to replace it with the Euler equations when the shock is not weak because the potential flow calculation may provide incorrect solutions.¹⁵

Even though some inverse methods for the two-dimensional Euler equations have been developed at transonic speeds, the existence and uniqueness problems of the inverse solutions have not been resolved because of the mathematical complexities in the formulation. In the three-dimensional case, the inverse solution existence problem is much less well developed, as discussed in Ref. 16. The question of well-posedness does not seem to have been addressed properly even for incompressible flow.¹⁶ One problem is that three-dimensional equivalents of Lighthill's constraints have not been formulated. Theoretical difficulties, however, do not prevent the development of useful inverse procedures.¹⁶

The purpose of this paper is to explore the existence and uniqueness problem for supersonic and hypersonic inverse solutions. As just mentioned, current two-dimensional inverse Euler methods and general three-dimensional inverse procedures do not have any mathematical or numerical criteria for the existence and uniqueness of the solution. However, useful predictions for the existence of the inverse solution and the verification of its uniqueness can be made for the three-dimensional inverse procedure⁴ developed for the Euler computer code¹⁷ and will be described.

Domain of Inverse Solution Existence

The recently developed three-dimensional inverse method⁴ assumes that space marching is valid for the supersonic and hypersonic freestream speed cases of interest. Thus, it steps one plane at a time using the same approach at each station. As pointed out in Ref. 3, the existence of the resulting body is not concerned a priori because the body shape is found at each marching plane, and the solution can simply be halted automatically if the specified pressure distribution leads to a body that would require a negative radius. Thus the target pressure distribution at a current computation station may be changed during the inverse iterations in case a negative body thickness is predicted.

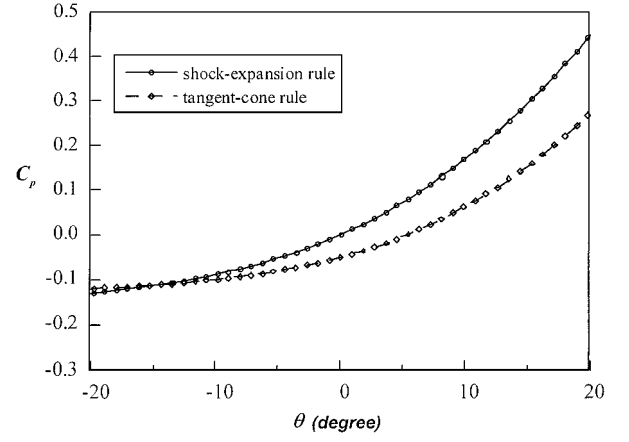
Although a general mathematical formulation or numerical criteria proving the existence of the inverse solution for the Euler equations in two-dimensional or three-dimensional problems is not available at present, the domain of inverse solution existence can be estimated for the supersonic and hypersonic bodies that employ space-marching techniques, with and without an angle of attack, using simple surface pressure/body shape rules.^{3,4} These rules can be used to establish an approximate connection between the change of surface deflection along a streamline and the change of pressure. Because the relation is approximate, an iterative procedure is used to obtain the exact connection between the geometry and pressure. However, the rules are sufficiently accurate to be used to establish limits for target pressures for which bodies with a thickness greater than zero exist. Two surface pressure/body geometry rules are considered next.

Shock-expansion pressure-shape rule¹⁷:

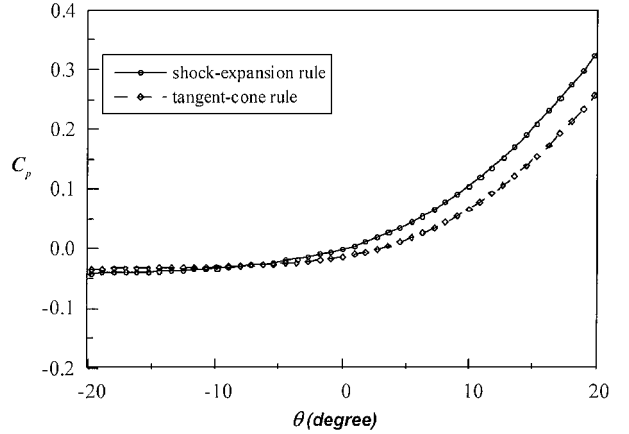
$$C_p = \frac{\gamma + 1}{2} m^2 \sin^2 \theta + \frac{2}{M_\infty} m \sin \theta \sqrt{1 + \left(\frac{\gamma + 1}{4}\right)^2 M_\infty^2 m^2 \sin^2 \theta} \quad (1)$$

where

$$m^2 = M_\infty^2 / (M_\infty^2 - 1) \quad (2)$$



a) Mach number = 3.0



b) Mach number = 6.0

Fig. 1 Pressure coefficient as a function of surface slope for two pressure-shape rules.

Tangent cone pressure-shape rule¹⁸:

$$C_p M_\infty^2 = \frac{4}{\gamma + 1} (k_0^2 - 1) + (k_0 - k_1)^2 \frac{2(\gamma + 1)k_0^2}{2 + (\gamma - 1)k_0^2} \quad (3)$$

where

$$k_1 = M_\infty \theta \quad (4)$$

$$k_0 = \frac{\gamma + 1}{\gamma + 3} k_1 + \sqrt{\left(\frac{\gamma + 1}{\gamma + 3}\right)^2 k_1^2 + \frac{2}{\gamma + 3}} \quad (5)$$

C_p is shown as a function of the body surface slope in Figs. 1a and 1b. At the higher Mach number they both produce similar results.

To establish the solution existence idea, consider each grid point in the current cross plane as a corresponding axisymmetric point that has the same z_i (z component at i th cross plane) and calculate the body slope angle θ_{extreme} that makes the thickness (or radius) zero. At every grid point j in the current cross plane i , this body-slope angle can be computed from

$$\tan \theta_j = \left(\frac{dz}{dx}\right)_j \approx \frac{(z_{i+1} - z_i)}{\Delta x_i} \geq \frac{(z_0 - z_i)_j}{\Delta x_i} \quad (6)$$

where z_0 is the reference point value (z_0 is set to zero for an uncambered geometry like an elliptic cone and is set to z value at y_{max} for a cambered geometry like a cambered wing or a hypersonic waverider). For each grid point in the i th cross plane, the surface pressure distribution greater than the pressure distribution at θ_{extreme} must be prescribed for an inverse solution to exist for all grid points in the current (i th) computational cross plane. The angle-of-attack effect must be considered when evaluating θ_{extreme} .

$$C_p(\theta) \geq C_p(\theta_{\text{extreme}}) \quad (7)$$

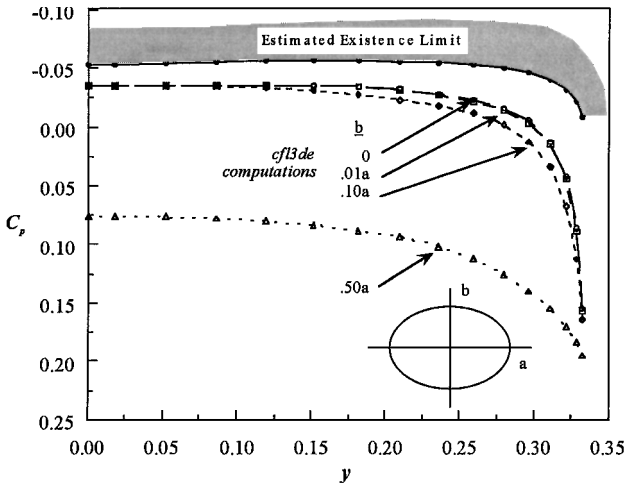


Fig. 2 Domain of existence: elliptic cone ($M_\infty = 6.28$, $\alpha = 0$ deg).

where, for the upper surface:

$$\theta_{\text{extreme}} = \tan^{-1}[(z_0 - z_i)/\Delta x_i] - \alpha \quad (8)$$

and for the lower surface:

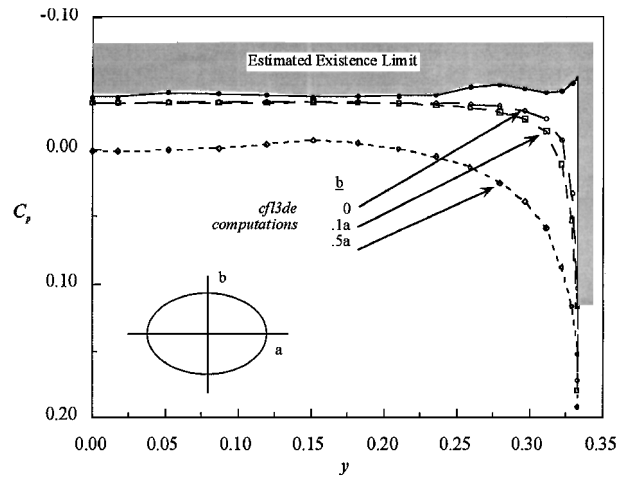
$$\theta_{\text{extreme}} = \tan^{-1}[(z_0 - z_i)/\Delta x_i] + \alpha \quad (9)$$

This approach is demonstrated through application to the elliptic cone and winglike nonconical cambered body, which were considered in the development of three-dimensional inverse procedure.⁴ CFL3DE (Ref. 19), which solves the Euler or thin-layer Navier-Stokes equations and is capable of treating general three-dimensional subsonic, transonic, supersonic, and hypersonic flow, was used to make the numerical calculations on the Virginia Polytechnic Institute and State University IBM 3090 computer. The code uses a cell-centered finite volume method employing flux-splitting schemes. Either a space-marching or a global iteration technique can be selected. For current study the space-marching method was used. A vertical plane of symmetry was assumed, and a grid of 31×20 (circumferentially and radially, respectively) was used. Numerous evaluations have verified the accuracy of this code, e.g., Ref. 20.

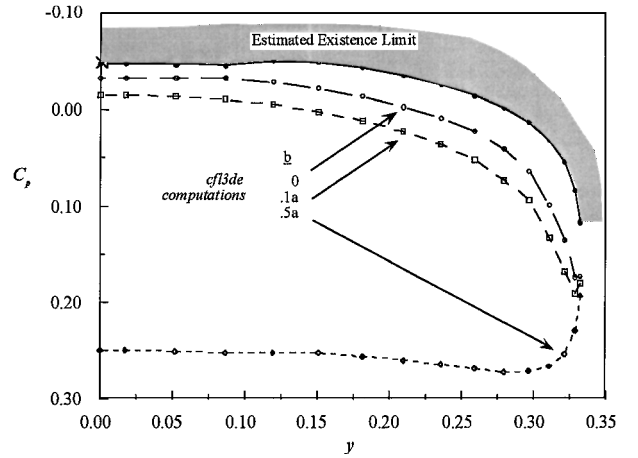
For several elliptic body shapes the limiting C_p distributions were estimated using the shock-expansion rules just given in Eq. (1) for $M_\infty = 6.28$ and zero angle of attack. As shown in Fig. 2, the predicted limit of C_p using Eq. (7) is less than the C_p of all of the body shapes, which were computed computationally using CFL3DE, including the body shape of zero thickness at the i th plane. Thus it appears that no target pressure distribution, which has a smaller value than the limit estimated from Eq. (7), will generate a physically realizable body shape. The same approach is also applied at $\alpha = 10$ deg. As shown in Fig. 3a for the upper surface and Fig. 3b for the lower surface, the same prediction for the target pressure distribution can be made in the presence of angle of attack. The upper-surface zero thickness computation is in very good agreement with the estimated limit for the pressure distribution existence.

For winglike nonconical cambered body shape, the C_p distribution was calculated for the body shape of zero thickness at the i th plane. The analysis results and the estimated limiting C_p distribution are compared in Fig. 4a for the upper surface and Fig. 4b for the lower surface. The result for the body shape considered in Ref. 4 is also included. The conclusion obtained for the elliptic cone test case remains valid for this body.

Although the prediction of the domain of inverse solution existence is limited to the space-marching problem at supersonic and hypersonic speeds, this approach is simple to apply, and it provides a necessary condition for the inverse solution existence without making any inverse calculations. This helps the designer to define the specification of the attainable target pressure distributions for supersonic and hypersonic body design.



a) Upper surface



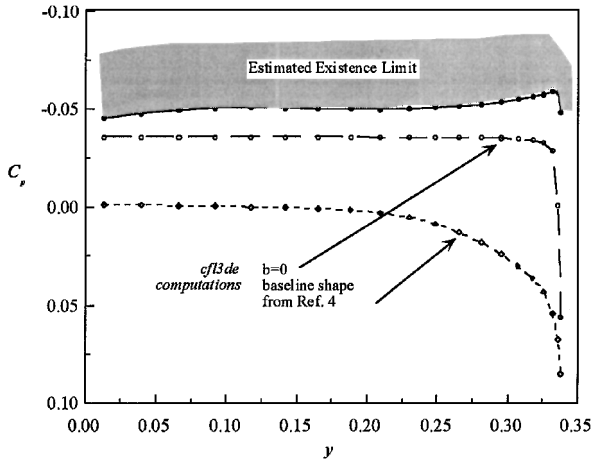
b) Lower surface

Fig. 3 Domain of existence: elliptic cone ($M_\infty = 6.28$, $\alpha = 10$ deg).

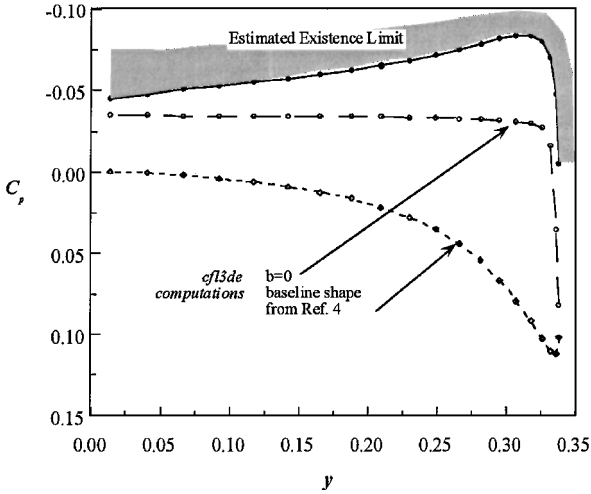
Inverse Solution Uniqueness

In the three-dimensional space-marching inverse procedure⁴ a pressure distribution specified according to the nondimensionalized y coordinate with respect to the semispan length a in the cross plane is used as a target pressure distribution. It is important to realize that the planform shape is to be found as part of the solution during the inverse iterations. In the three-dimensional inverse examples presented in Ref. 4, a unique body geometry was found, independent of the several different guesses for the initial body geometry. This leads to the following question: Can a converged body geometry be obtained by correcting just the contour distribution, i.e., by changing the cross-sectional shape while maintaining the semispan length in the cross plane? In other words, is the body shape unique which satisfies both the target pressure specified according to the nondimensionalized span location and the previous cross-plane data? The question is basically a problem of the inverse solution uniqueness. A special consideration in three-dimensional supersonic and hypersonic flow is the issue of downstream influence of the flowfield at a particular crossflow plane.

In inviscid flow there may exist numerous solutions that satisfy the target pressure distribution specified according to the nondimensionalized coordinate y/a by similarity. (At the same freestream condition, similar body shapes produce the same pressure distribution according to the nondimensionalized coordinate y/a .) Thus, an infinite number of body shapes can be generated for the given target pressure distribution based on the nondimensionalized y/a coordinate. Even though the cross-sectional shape of a three-dimensional body is similar in concept to the shape in two dimensions, especially when the space-marching numerical technique is employed, there is an influence from the preceding data plane on the present plane. That means, the inverse solution (section geometry) in the current plane is dependent not only on the pressure distribution according to the



a) Upper surface



b) Lower surface

Fig. 4 Domain of existence: nonconical cambered body ($M_\infty = 6.28$, $\alpha = 0$ deg).

nondimensionalized span location, but also on solutions at the preceding plane. This is a general characteristic in three-dimensional flow. In analysis solutions the flow properties in the present cross plane are dependent upon both the solution at the preceding plane and the body geometry data in the current plane.

In two-dimensional or axisymmetric flow a new grid point z_i (body radius at i th cross plane) is determined by the surface slope angle at the current cross plane and z_{i-1} (body radius at $i-1$ st plane). z_{i-1} is known from the geometry data at the preceding plane, and the surface slope angle is determined by the specified pressure using a surface pressure-body geometry rule.^{3,4} If C_p is a single-valued function of surface slope θ , only one value of θ will be found from the specified pressure coefficient. Then the body geometry point z_i is uniquely determined. If the surface pressure-body geometry rule is exact, a unique body shape will be found without any inverse iterations.

Thus, it is necessary to consider the relation between the surface pressure and body slope angle θ to show the uniqueness of the solution. The first step is to show that $C_p(\theta)$ is a single-valued function of θ . As can be seen in the Fig. 1, only one value of θ is matched for the given surface pressure coefficient for both supersonic and hypersonic speeds. The basic idea of the three-dimensional space-marching inverse procedure⁴ is to apply the surface pressure/body geometry rules^{3,4} along the surface streamline. The surface geometry is then adjusted in the plane of the surface streamline (the plane which encloses the points A, B, C in Fig. 5). From the C_p - θ relation, there is only one body surface slope θ for the given C_p , which implies that a new body geometry at the present computational plane (i th plane) is uniquely determined by the body geometry and flow data at $i-1$ st plane and the body surface slope θ .

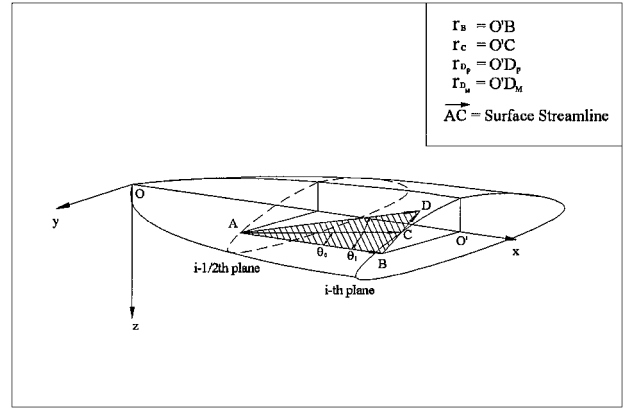
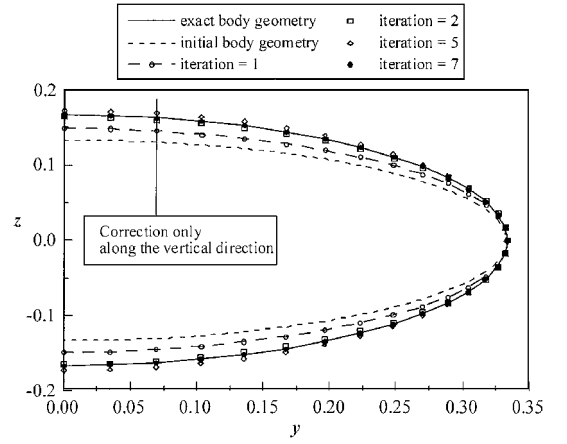


Fig. 5 Body-geometry definition and the shape correction along the surface streamline.

Fig. 6 Effect of fixed planform: body-geometry convergence of the elliptic cone ($M_\infty = 6.28$, $\alpha = 0$ deg).

In Fig. 5 AC is the surface streamline that passes through the given point A. C is the intersection point of the surface streamline to the vertical plane of the i th station. (Points B, C, and θ_i are determined by solutions of the preceding plane. Only one value of θ_i is obtained by the pressure-body shape rule.) Using this information, the new surface point D is uniquely determined. The distances from the x axis are calculated for points B, C, D_p , and D_M . These distances are denoted by r_B , r_C , r_{D_p} , r_{D_M} , respectively. By comparing r_{D_p} , r_{D_M} with r_B and by considering the sign of θ_i , either D_p or D_M is selected as a new body point.³ The details are described in Ref. 4.

As the inverse iteration continues, ΔC_p (the difference between the target pressure coefficient and the calculated pressure coefficient) is decreasing, and the body shape goes to the exact one. The planform-shape modification y_{\max} is exactly the same procedure as with the points at C and D.

Because the inverse solution that satisfies both the target pressure distribution and the preceding cross-plane data is unique as already explained, the same inverse solution must be obtained regardless of the initial guesses for the body geometry. In Ref. 4 numerous inverse calculations were made for the elliptic cone with different initial guesses. As the desired body geometry (i.e., inverse solution) is unique, the corresponding y_{\max} point is also unique. Thus, if the initially assumed y_{\max} point happens to be the same with the desired (or exact) y_{\max} point, the point should not move during the inverse iteration for the solution to be unique. Even though the developed inverse method⁴ allows for the body points to move to any direction, the body geometry must be modified only along the vertical direction because the planform shape (y_{\max} point) will not be changed during the inverse iterations. To check whether the three-dimensional inverse procedure⁴ has the aforementioned behavior, which implies the uniqueness of the solution, a sample inverse calculation is performed for the elliptic cone test case. The initial body geometry has an exact planform shape and a different thickness distribution along the cross plane as shown in Fig. 6. Even though no

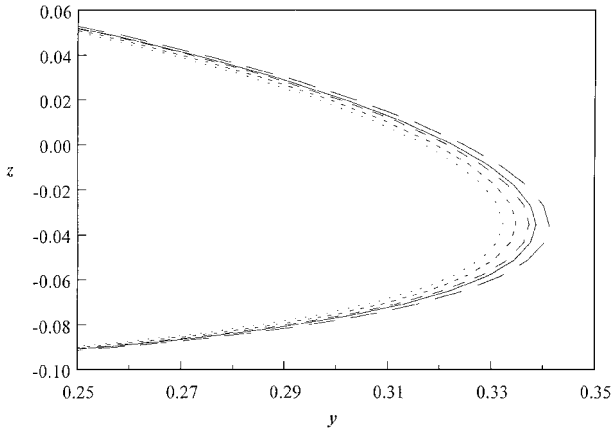


Fig. 7 Winglike nonconical cambered body with different semispan lengths.

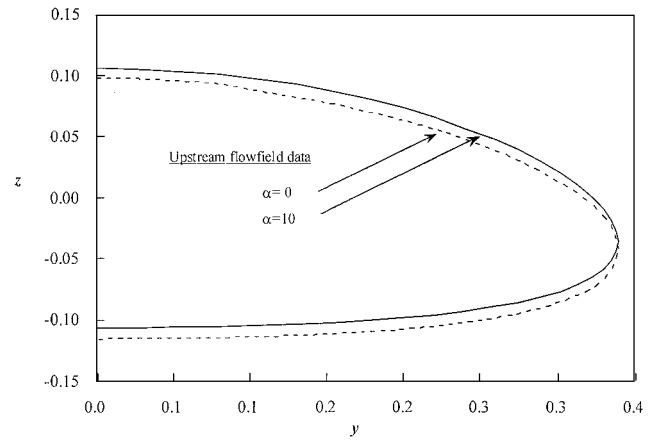
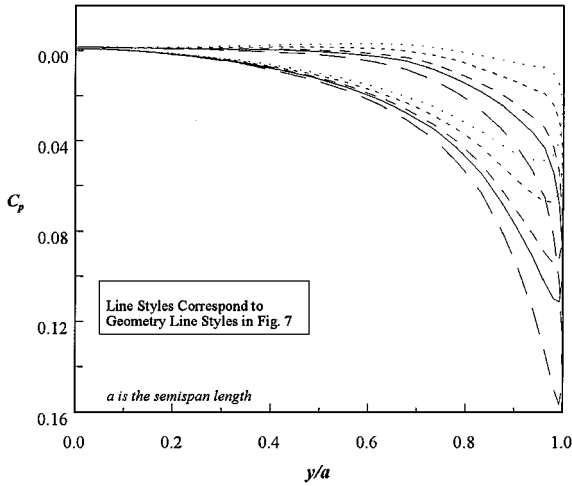
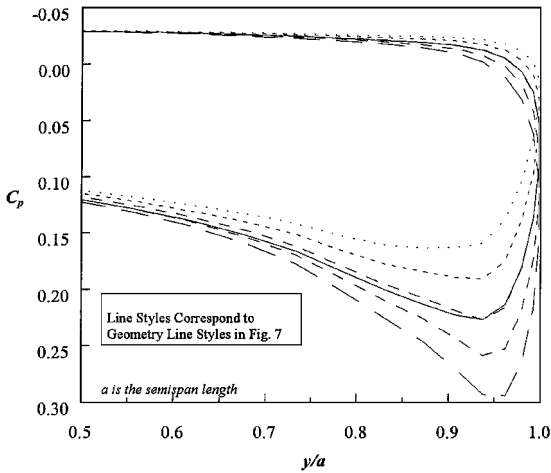


Fig. 9 Inverse solution uniqueness: effect of upstream flowfield ($M_\infty = 6.28$, $\alpha = 0$ deg).



a) $M_\infty = 6.28$, $\alpha = 0$ deg



b) $M_\infty = 6.28$, $\alpha = 10$ deg

Fig. 8 Several pressure distributions with different semispan lengths in winglike nonconical cambered body.

restriction to the direction of body-shape correction is given, the behavior is similar to the case with fixed planform, and a converged body geometry is found within seven inverse iterations. The body geometry convergence is shown in Fig. 6.

However, in general, the planform shape y_{\max} that satisfies a given target pressure distribution is not known until an inverse calculation is performed. Thus, in case the planform shape is prescribed as a design requirement, an understanding of the effect of the target pressure selection on the resulting planform shape is needed. The target pressure distribution may have to be modified during the inverse

iterations to satisfy the given planform shape. This consideration may lead naturally to a combination of optimization and inverse method already used in transonic design but equally applicable to the current class of design problems known as Smart Aerodynamic Optimization.²¹

The effect of the target pressure selection on the planform shape is investigated for the winglike nonconical cambered body.⁴ Body shapes, which are different mainly in semispan length, are calculated at $M_\infty = 6.28$, as shown in Fig. 7. The corresponding differences of the pressure distributions are clearly shown in Figs. 8a and 8b with and without the angle of attack. Even though these body shapes are three-dimensional, the local changes of the body shapes result in local changes of corresponding pressure distributions as can be seen in the figures. Thus, by adjusting the target pressure distribution near $y/a = 1.0$ (a is semispan length), a body shape that has a different semispan length can be generated. This type of knowledge is useful for practical aerodynamic design problems. By modifying the target pressure distribution specified according to nondimensionalized coordinate y/a during the inverse iterations, the developed three-dimensional inverse method can be applicable to the design problem of a fixed planform shape.

One other example calculation is performed for the same body considered above at $\alpha = 10$ deg to illustrate the uniqueness of the inverse solution and the connection with the upstream data plane. Two different flowfield solutions are used as data in the preceding plane (solutions for $\alpha = 0$ and 10 deg), and two inverse solutions are computed, each using the same target pressure distribution. The results are shown in Fig. 9. As expected, the use of different data in the preceding plane results in different body shapes for the same target pressure distribution at the current station.

Conclusions

For the three-dimensional inverse problems employing the space-marching technique, the following conclusions about the inverse solution existence and uniqueness can be made. By using extreme body-slope angle, a simple method to predict the domain of the inverse solution existence has been proposed and applied to several example test cases with and without angle of attack. It gives useful information about inverse solution existence without requiring an inverse calculation. By investigating the relations between the surface pressure and the body geometry, a general explanation for the inverse solution uniqueness has been described. Sample calculations to support this explanation have been presented.

Acknowledgment

We would like to acknowledge R. W. Walters for providing us with access to CFL3DE.

References

- Scott, W. B., Dornheim, M. A., Smith, B. A., and Ott, J., "The Future of High-Speed Flight," *Aviation Week and Space Technology*, 13 Oct. 1997, pp. 62-76.

²Caceres, M. A., "Launch Vehicles: Mostly Thriving," *Aviation Week and Space Technology*, 12 Jan. 1998, pp. 125, 126.

³Lee, Jae-Woo, and Mason, W. H., "Development of an Efficient Inverse Method for Supersonic and Hypersonic Body Design," *Journal of Spacecraft and Rockets*, Vol. 31, No. 3, 1994, pp. 400-405.

⁴Lee, Jae-Woo, and Mason, W. H., "New Three-Dimensional Inverse Method for High-Speed Vehicle Design," *Journal of Spacecraft and Rockets*, Vol. 35, No. 4, 1998, pp. 473-479.

⁵Lighthill, M. J., "A New Method of Two-Dimensional Aerodynamic Design," Aeronautical Research Council, Repts. and Memoranda 2112, London, April 1945.

⁶Woods, L. C., "The Design of Two Dimensional Aerofoils with Mixed Boundary Conditions," *Journal of Quarterly Applied Mathematics*, Vol. 13, No. 2, 1955, pp. 139-146.

⁷Volpe, G., and Melnik, R. E., "The Design of Transonic Aerofoils by a Well-Posed Inverse Method," *International Journal for Numerical Methods in Engineering*, Vol. 22, No. 2, 1986, pp. 341-361.

⁸Volpe, G., and Melnik, R. E., "The Role of Constraints in the Inverse Design Problem for Transonic Airfoils," AIAA Paper 81-1233, June 1981.

⁹Volpe, G., "The Inverse Design of Closed Airfoils in Transonic Flow," AIAA Paper 83-0504, Jan. 1983.

¹⁰Daripa, P., "An Exact Inverse Method for Subsonic Flows," *Quarterly of Applied Mathematics*, Vol. 46, No. 3, 1988, pp. 505-526.

¹¹Gally, T. A., and Carlson, L. A., "Inviscid Transonic Wing Design Using Inverse Methods in Curvilinear Coordinates," AIAA Paper 87-2551, 1987.

¹²Weed, R. A., Anderson, W. K., and Carlson, L. A., "A Direct-Inverse Three Dimensional Transonic Wing Design Method for Vector Computers," AIAA Paper 84-2156, Aug. 1984.

¹³Shankar, V., "Computational Transonic Inverse Procedure for Wing Design with Automatic Trailing Edge Closure," AIAA Paper 80-1390, July 1980.

¹⁴Moretti, G., "Considerations on Existence and Uniqueness in Numerical Inverse Design," *Proceedings of the First International Conference on Inverse Design Concepts in Engineering Science*, edited by G. S. Dulikravich, Univ. of Texas, Austin, TX, 1984, pp. 68-83.

¹⁵Salas, M. D., Jameson, A., and Melnik, R. E., "A Comparative Study of the Non-Uniqueness Problem of the Potential Equation," AIAA Paper 83-1888, July 1983.

¹⁶Slooff, J. W., "A Survey of Computational Methods for Subsonic and Transonic Aerodynamic Design," *Proceedings of the First International Conference on Inverse Design Concepts in Engineering Science*, edited by G. S. Dulikravich, Univ. of Texas, Austin, TX, 1984, pp. 1-67.

¹⁷Carafoli, E., *Wing Theory in Supersonic Flow*, Pergamon, Oxford, 1969, pp. 463-473.

¹⁸Krasnov, N. F., *Aerodynamics of Bodies of Revolution*, Elsevier, New York, 1970, pp. 463-470.

¹⁹Thomas, J. L., van Leer, B., and Walters, R. W., "Implicit Flux-Split Schemes for the Euler Equations," AIAA Paper 85-1680, July 1985.

²⁰Mason, W. H., and Lee, Jae-Woo, "Minimum Drag Axisymmetric Bodies in the Supersonic/Hypersonic Flow Regimes," *Journal of Spacecraft and Rockets*, Vol. 31, No. 3, 1994, pp. 406-413.

²¹Aidala, P. V., Davis, W. H., Jr., and Mason, W. H., "Smart Aerodynamic Optimization," AIAA Paper 83-1863, July 1983.

J. Kallinderis
Associate Editor